Crystallization of Sol-Gel Derived Lead Zirconate Titanate Thin Films in Argon and Oxygen Atmospheres

L.A. Bursill* and Keith G. Brooks

Laboratoire de Ceramique, MX-D, Ecole Polytechnique Federale de Lausanne, Ecublens, CH-1015, Suisse

* Permanent Address:
School of Physics, The University of Melbourne Parkville, 3052, Vic., Australia

Received to be inserted
Revised to be inserted

Abstract

Electron diffraction and high-resolution electron microscopic techniques are applied to reveal the mechanisms of crystallization of 75nm thin films of ferroelectric lead-zirconate-titanate (PZT). Sol-gel methods, followed by pyrolysis at 350degC, were used to provide a common starting point after which a variety of rapid-thermal annealing (RTA) experiments in the temperature range 400-700degC were made in argon, oxygen and nitrogen/hydrogen atmospheres. The results are interpreted in terms of a crystal chemical analysis, which points out that partial pressure of oxygen and heating rate are important experimental parameters which must be controlled if ferroelectric perovskite-type Pb_2ZrTiO_6, rather than pyrochlore-type Pb_2ZrTiO_{6+X}, where $0 < X < 1$ or $-1 < X < 0$, is to be obtained after the RTA step. Thus significant improvements in the crystallization of perovskite-type PZT were clearly demonstrated by using argon atmospheres for the RTA step.

The results have significance for the production of high-quality ferroelectric thin films, with improved switching and fatigue characteristics, since even small amounts of the pyrochlore phase prove detrimental for these properties.

I. INTRODUCTION

Lead-zirconate-titanate (PZT) ferroelectric thin films have been produced by a variety of sol-gel processes[1-3]. Interest centers on their remanent polarization, coercive field and fatigue characteristics for their potential application in high density dynamic random-access memory (DRAM) capacitors, nonvolatile memories or micro-manipulation devices. The as-deposited films are amorphous and annealing in the temperature range 350-700degC is required to crystallize the ferroelectric perovskite structure of PZT. In general the amorphous phase transforms first to a metastable pyrochlore-type structure (350-500degC) which may then crystallize as stable perovskite (500-700degC)[4]. The annealing may be done in a furnace for up to 30mn or preferably, for VLSI intergration, by rapid- thermal-annealing (RTA) for 30-60s. Recent studies of a large number of PZT thin films, from a wide range of sources, including many made in-house, have shown that even small remanent nanoscale crystallites or layers of pyrochlore are detrimental to the electrical and fatigue characteristics[5].

There have been no reports of explicit attempts to control the formation of the pyrochlore phase. However, some authors have reported crystallization of ferroelectric PZT at temperatures as low as 450degC, possibly without a pyrochlore intermediate phase[3,6]. Thus Hirano et al[3] obtained interesting results using wet oxygen, rather than air during annealing.

Some consideration of crystal chemical data, especially the oxidation state of lead after pyrolysis and during annealing in the temperature range 350-700degC, immediately suggests that there will a Pb^{4+} component, variably depending on the temperature, heating rate and duration, the nature of the substrate and most importantly on the partial pressure of oxygen.

This paper gives first a brief crystal chemical argument, pointing out why the pyrochlore phase may be stabilized at the expense of perovskite; then a set of experiments is described which show that annealing in argon may be used to control, to some significant extent, the crystallization of pyrochlore and/or perovskite PZT. Annealing in oxygen favours the pyrochlore structure to such an extent that it may remain such even on annealing at 700degC.

II. SOME CRYSTAL CHEMICAL PRINCIPLES.

(a) Stability of lead oxides.

The Pb-O system has a rich phase structure, as revealed by the fundamental studies of Anderson and Sterns[7], White and Roy[8], Sorrel[9] and Kovtunenko, Kharif, Nesterova and Stupak[10]. Of special interest

here is the stability of lead oxides in the range PbO-Pb_3O_4 in air and for the temperature range 350-700degC. Sorrel made a remarkably thorough study of oxidation/reduction kinetics in just this range. From his work and from the thermodynamic study of Kovtunenko et al it is clear that PbO will tend to oxidize when heated in air at 300-450degC but continued heating at 450-700degC will tend finally to reduce PbO_{1+x} back towards PbO. The final stoichiometry will thus depend to a large extent on details of the annealing path and partial pressure of oxygen, i.e. on the kinetics of the annealing path. The fundamental reasons for this point appear to have escaped previous workers in this field. Of course we are now dealing with the more complex system PbO/$PbZrO_3$/$PbTiO_3$, the RTA process occurs at a very different rate and the crystallization is occurring on a Pt/Ti/SiO2/Si substrate in most cases of interest for ferroelectric thin film properties. par It is not certain what is the mean oxidation state of Pb after pyrolysis of the air-dried precursor sol-gel at say 350degC. Let us assume, for simplicity, that this may be made to be exactly Pb^{2+}, by control of the sol-gel solution chemistry. Then during RTA, or other annealing experiments, such as furnace heating in air, the oxidation state will tend to shift upwards so that Pb^{4+} ions will coexist with Pb^{2+}. The overall stoichiometry, in particular, oxygen content, will therefore change to something like Pb_2ZrTiO_{6+X}, where $0 < X < 1$. (Here we have not included any excess PbO which may have been added, apparently to compensate for "Pb-loss" during annealing. We return to discuss this point in sec.5 below.)

White and Roy[8] studied the phase relations for the system Pb-O in the pressure range 3-1400bars over the temperature range 200-900degC. This is mostly out of the present ranges of interest; however, they did make the interesting remark that "Pb_3O_4 heated to about 700degC in an open crucible in air was observed to react to PbO in less than about 30 seconds. This is just the order of magnitude of reaction speed commonly found appropriate for RTA of sol-gel PZT thin films.

Of more direct relevance is the work of Kovtunenko et al[10], who measured the solubility of oxygen in PbO in the range 500-750degC at oxygen pressures between 2-730mmHg. Their results were expressed as two equations describing the solidus line bounding the region of homogeneity of PbO on the Pb_3O_4 side. Thus the equilibrium partial pressure of oxygen over solid PbO and Pb_3O_4 is described by

$$p_{O_2}(atm) = \exp(-8440/T + 9.864) \tag{1}$$

and the solubility of oxygen in PbO, written as $PbO_{1+O(x)}$, is given by

$$O(x)(g - atomO/molePbO) = \exp(-4220/T + 0.94) \tag{2}$$

These two results are shown plotted in Fig.1a,b respectively.

Note especially the following points; PbO and Pb_3O_4 coexist up to 550-600degC in oxygen at 1atm, up to 450-500degC in air (0.25atm oxygen) but up to only about 300-350degC for $pO_2 = 0.01$atm. In order to ensure only Pb^{2+} ions, i.e. Pb as $PbO_{1.00}$, we may require $pO_2 < 10^{-3}$atm throughout the temperature range 300-600degC.

Of course the above results may not translate directly into the more complex $PbO/PbZrO_3/PbTiO_3$ system, plus any remaining by-products of the sol-gel pyroysis. However, it is reasonable to assume that those results will lie at the core of any changes of stoichiometry; in particular the oxidation state of Pb and the consequent oxygen stoichiometry of the complex oxides produced by RTA in the range 350-700degC.

We conclude this section by asserting that it should be possible to control the oxygen content by doing the RTA in approx. 10^{-3}atm oxygen. The reasons why this should be critical for obtaining crystallization of perovskite, rather than pyrochlore, are addressed in the next section.

(b) Crystal Chemistry of Perovskite and Pyrochlore Formation.

It is important to note, first of all, that the perovskite structure, mostly written ABO_3, is usually formed as a stoichiometric oxide; it is not recognized as a nonstoichiometric oxide, in the sense that the occupancy of the 12-coordinated A site, of the 6-coordinated B sites or of the O sites readily depart from unity. In the case considered here we expect therefore that the PZT perovskite phase will be Pb_2ZrTiO_6, with departures of occupancies of less than say 1 to 2at. percent. Thus, we predict that if amorphous PZT is to crystallize rapidly with the perovskite structure, in a controlled, reproducible manner, then the as pyrolyzed films should have exactly this stoichiometry and, furthermore, it is preferable to retain that stoichiometry during the RTA. Most authors on the subject have implicitly made this assumption, although there have been few, if any, attempts to check that this actually occurred during processing. Trial and error methods have predominated and results have not always been reproducible from laboratory to laboratory. It is remarkable that quite useful PZT thin films have been obtained, although behaviour has not been totally reproducible and probably the electrical properties have not yet been optimized.

Pyrochlore is well known to exhibit quite wide ranges of stoichiometry; it is a typical nonstoichiometric oxide[11]. Ideally, this structure type is written, $A_2B_2O_7$. However, the oxygen content may be as low as O_6, as reported for $Pb_2Ti_2O_6$ (Martin[12]), assuming valence states Pb^{2+} and Ti^{4+}. For the $PbO\text{-}Nb_2O_5$ system pyrochlore structures were found to exist for $3PbO\text{-}2Nb_2O_5$, $2PbO\text{-}Nb_2O_5$, $3PbO\text{-}Nb_2O_5$ and $5PbO\text{-}2Nb_2O_5$ (Chaput, Boilot Lejeune, Papiernik and Hubert-Pfalzgraf[13]). The first of these may be

described as an A-deficient pyrochlore with formula $Pb_{1.5}Nb_2O_{6.5}$. The second is simply stoichiometric pyrochlore $Pb_2Nb_2O_7$ whereas the third and fourth variations may be described as B-deficient pyrochlores $Pb_2Nb_{1.33}O_{5.33}$ and $Pb_2Nb_{1.6}O_6$ respectively. Although full phase and structural studies do not exist for pyrochlore phases of the PbO-$PbZrO_3$-$PbTiO_3$ system it is apparent that they certainly exist. We assert therefore that the presence of excess- or deficient- PbO, the presence of Pb^{4+} and/or the presence of oxygen stoichiometry $>O_6$ or $<O_6$ will all favour the formation of more or less stable pyrochlore phases. Thus if the stoichiometry, including both the Pb and O content, is not controlled at or after pyrolysis and during RTA it is likely to be more difficult to go directly to the stoichiometric perovskite PZT structure.

It is on the strength of the arguments of the preceeding two paragraphs that we designed the experiments reported below. Thus we searched for different crystallization phenonema for sol-gel derived PZT thin films given RTA in flowing argon, which should favour perovskite, compared with films given RTA in flowing oxygen, which should favour pyrochlore. Some experiments were also made using an atmosphere of forming gas ($95\%N_2/5\%H_2$) during thermal annealing. The latter should provide somewhat more severe reducing conditions.

III. EXPERIMENTAL.

(a) Film Preparation.

PZT films were made using a modification of the sol-gel process first reported by Budd, Dey and Payne[14]. The organometallic precursor solutions were not prehydrolyzed in our work. $Pb(C_2H_4O_2).3H_2O$ was dissolved in 2-methoxyethanol. Vacuum distillation was used to remove the water associated with the hydrated Pb salt. A solution of Zr-n-propoxide and Ti-propoxide in 2-methoxyethanol was then added to the Pb precursor solution and refluxed for 2 hours. A solution containing the equivalent of 0.4 moles of $Pb(Zr_{0.53}Ti_{0.47})O_3$ per liter of solution was obtained by further distillation. The quantity of $Pb(C_2H_4O_2).3H_2O$ was calculated to include 10% excess PbO. Other reaction by products were also removed from the sol-gel stock solution during this vacuum distillation process (Dekleva, Hayes, Cross and Geoffrey[15]). A microprocessor-controlled vacuum distillation apparatus (Rotavapor EL-141, Buchi Laboratory-Techniques, Inc., Flawil, Switzerland) was used to achieve reproducibility of solution preparation.

PZT precursor thin films were prepared by coating the stock solution (diluted to 0.062M) directly onto 400 mesh 3.2mm platinum electron microscope specimen support grids. We note that a similar technique for preparing specimens suitable for transmission electron microscopy was first reported by

Kwok and Desu[16] ; our technique developed quite independently of them and was designed specifically to provide very thin specimens (less that 10um thick) as required for atomic resolution transmission electron microscopy; in particular ion-beam thinning was explicitly eliminated from the technique to avoid production of amorphous layers on the surface of the specimens.

Results from eleven films are reported below; they were given pyrolysis and RTA treatments as indicated in Table 1. The first specimen studied (specimen A) was simply dried in air and then given RTA at 700degC for 1 min in air. It contained only pyrochlore, as described in the results section below. This was a surprising result, since PZT thin films prepared from the same sol-gel precursor solution gave crystalline perovskite phase when deposited on $Pt/Ti/SiO_2/Si$ substrates followed by RTA at 700degC for 1 min[5]. It was this observation which lead to the present investigation of the effect of RTA atmosphere, specifically the effect of partial pressure of oxygen on the relative stabilities of the pyrochlore and perovskite structures of PZT.

These different peparations were designed to test for the effect of oxidation state of Pb on the crystallization. A typical RTA profile consisted of heating from room temperature to e.g. 600degC at approx. 60degC/s, holding at temperature for 1 min and then cooling to room temperature by extinguishing the quartz lamp.

The as grown films were discontinuous, as shown by optical microscopy. Thus the films grew attached to the platinum grid, but did not extend fully across the space between grid bars. The overall film thickness was estimated to be about 75nm.

(b) Electron Microscopy.

The specimen grids were examined directly without need for further thinning using a Philips EM430 300KeV electron microscope at Institut Interdepartementale de Microscopie Electronique (I2M), EPFL. Observations were made at close to room temperature using a +/- 10 deg double-tilt goniometer. The instrumental resolution was significantly better than 0.2nm although the interpretable structure resolution was limited to 0.2nm, since the spherical aberation coefficient was 1.2mm. Selected area diffraction patterns were recorded using the smallest projector lens aperture, when the effective beam diameter at the specimen plane was about 100nm. HRTEM and electron diffraction observations were made from the thin edges of the films (thickness 1-20nm say).

IV. RESULTS.

(a) Specimen A. RTA 700degC in air.

Figs.2a,b show a typical electron diffraction pattern and the corresponding HRTEM image. This specimen is polycrystalline on the nanoscale; it consists of randomly oriented crystallites < 7nm in diameter. The electron diffraction ring pattern was indexed as cubic pyrochlore-type (a = 1.06nm); it appears virtually identical to patterns published by Klee et al[2] and also by Kwok and Desu[16] . It is also quite consistent with many of the the XRD powder patterns published in the literature relating to PZT thin film processing in the past 2-5 years see e.g.[2,3,6,17]. In fact we simulated by computer calculations electron diffraction powder patterns for all the lead oxides, zirconium titanates, lead titanates and lead zirconate-titanates recorded in the ASTM powder data files and came to the independent conclusion that a cubic pyrochlore-type structure is the only reasonable fit. We will refer to this structure as $Pb_2(Zr,Ti)O_{6+x}$, where $0< x < 1$. Attempts to recrystallize this specimen by use of excessive electron beam currents were made but, in this case, the specimen proved to be very stable.

Note that occasionally individual nanocrystals were oriented close to the [100], [110] or [111] principal zone axes of the cubic pyrochlore structure (see Fig.2b), when two-dimensional HRTEM images were obtained. Note that there appears to be some remanent amorphous or very poorly crystallized material, even after RTA at 700degC for this specimen. On the other hand, spot patterns sometimes showed 111 reflections of the perovskite phase. However the bulk of this specimen was stuck in the pyrochlore structure. As an aside we note that a pellet 3mm diameter by 2mm deep, made from this same sol-gel precursor was annealed in air at 1200degC for 2 hours. This also contained mostly pyrochlore phase. Only after annealing at 1250degC for 48 hours was this pellet substantially converted to perovskite PZT.

(b) Specimen B. No RTA 350degC pyrolysis only.

Figs.3a,b are an electron diffraction pattern and corresponding typical HRTEM image of the as-pyrolysed specimen B. This specimen was totally amorphous, as expected. Note the broad diffuse ring pattern (Fig.3a), whose first strong ring sits over the intense 222 ring of the pyrochlore pattern (cf. Fig.2a). The second weak diffuse ring also sits over the next most intense rings of the pyrochlore-type structure. This specimen was also remarkably stable under electron beam irradiation. The HRTEM images showed no evidence for incipient crystallization at this stage.

(c) Specimen C. RTA 600degC in argon.

Figs.4a,b show a typical electron diffraction pattern and the corresponding HRTEM image of this specimen, which was annealed in flowing argon. Relatively large crytallites, 20-50nm diameter, of perovskite-type PZT were obtained. In the case shown as Fig.4b the crystallite is oriented along a [110] zone axis; there is some evidence, in the form of variations in fringe intensity and continuity that the perovskite may contain an incompletely ordered distribution of Zr and Ti atoms over the perovskite B sites due to inhomogeneities in the Zr,Ti distribution existing in the original pyrolysed material. This statement may be made after comparing the image quality with images obtained from other PZT specimens we have studied, including high density ceramic specimens which gave perfectly regular HRTEM images for the same imaging conditions (Bursill, unpublished results, 1992/1993).

The electron diffraction patterns (Fig.4a) were indexed readily as perovskite (cubic, a = 0.40nm). Note that the strongest pyrochlore ring is just visible in Fig.4a, consistent with slightly less than 100 percent crystallization as perovskite.

(d) Specimen D. RTA 600deg in oxygen.

Figs.5a,b give the corresponding results for specimen D, which was annealed in flowing oxygen. Note the continuous ring pattern characteristic of pyrochlore structure (Fig.5a) and the poorly nanocrystalline structure shown in the HRTEM image (Fig.5b). In this case there is short-range order in the pyrochlore on the scale of only 10 lattice spacings, which is significantly less than for wever in this case specimen A.

(e) Specimen E. No RTA 420deg pyrolysis only.

This specimen was virtualiy identical to Specimen B; Figs. 6a,b show the corresponding electron diffraction pattern and HRTEM image respectively. The diffuse ring patterns may be somewhat less broad than Fig.3a; however, there was no significant crystallization evident in the HRTEM images. It is worth noting that this specimen was slightly beam sensitive in that rafts consisting of one or two atomic layers closely ressembling the structure image of perovskite appeared after 20min obsevvation in the electron microscope (see Fig. 6c); in addition roughly spherical nanocrystallites (3nm diameter) appeared after about 20min observation under electron irradiation (see Fig.6c).

(f) Specimen F. RTA 400deg in argon.

This specimen was indistinguishable from the as pyrolysed specimen (cf. Fig.3).

(g) Specimen G. RTA 450deg in argon.

This specimen was interesting because it showed a variety of electron diffraction patterns. Fig. 7a shows a relatively very diffuse nanocrystalline pyrochlore pattern plus spot patterns which were indexed using the unit cell parameters of perovskite-type PZT. In other cases (Fig. 7b) single crystal perovskite spot patterns coexist with as-pyrolyzed type patterns. Here the [101] zone axis of perovskite was dominant. Fig.7(c) shows the HRTEM image from the corresponding area; this is a relatively large crystallite (say approx. 60nm diameter). This crystal is decorated by nanocrystals about 2-5 nm diameter; the fringe spacings of which are not consistent with perovskite- or pyrochlore-type PZT structure, but are consistent with PbO. The corresponding electron diffraction pattern (Fig.7b) also contains some PbO spots.

(h) Specimen H. RTA 500deg in argon.

This specimen showed electron diffraction patterns similar to those just described for specimen G; thus both amorphous as-pyrolyzed and nanocrystalline pyrochlore-type diffuse ring patterns occurred (Figs.8a,b). However the nature of the superimposed single crystal spot patterns changed, with pyrochlore-type spots replacing the perovskite-type spots of Fig.7a,b.

(i) Specimen I. RTA 550deg in argon.

It was remarkable that this specimen showed only nanocrystalline pyrochlore-type diffraction patterns (Fig.9); the pyrochlore nanocrystallite size size was relatively large, i.e. about the same size as for specimen A, cf. Fig.2b.

(j) Specimen J. RTA 600deg in forming gas.

This specimen showed only electron diffraction patterns of the type found for the as-pyrolyzed specimens B and E (see Fig. 10a). The corresponding HRTEM image was indistinguishable from that of the as-pyrolyzed specimen B (cf. Fig. 3b). There was no evidence for significant crystallization of

perovskite-type PZT. Weak spots did occur which coincided with the pyrochlore rings.

(k) Specimen K. RTA 450deg in forming gas.

This specimen gave electron diffraction patterns (Fig.10b) which were almost identical to Specimen J. There was no evidence for even partial crystallization towards perovskite- or pyrochlore-type PZT. The corresponding HRTEM image was essentially indistinguishable from that shown by the as-pyrolyzed specimen B (cf. Fig. 3b).

V. DISCUSSION.

It should be clear, from the results for specimens C and D, that RTA in argon at 600degC improved the crystallization kinetics to a remarkable extent compared to RTA in oxygen at 600degC; this is the most important observation. All of the remaining results (specimens A,B and E to K) are consistent with the expectations of section II above, i.e. that if the atmosphere is too rich, or poor, in oxygen then the resulting stoichiometry at the RTA step will be different than Pb_2ZrTiO_6 and the result may be essentially pyrochlore Pb_2ZrTiO_{6+X}, where $0 < X < 1$ or $-1 < X < 0$. Perovskite PZT is most likely to form during RTA only if x= 0.00.

The series E, F, G, H, C (all initially pyrolysed in air at 350degC then given RTA at 400-600degC in 50degC intervals) offers considerable insight into the crystallization mechanisms involved. Note that crystallization of perovskite was initiated at 450degC (Fig.7) but was incomplete. RTA at 500degC and 550degC gave suprisingly pyrochlore, rather than perovskite crystallization. RTA at 600degC did however produce predominantly perovskite type PZT. These results may be understood if the heating rate as well as RTA temperature are significant; thus heating at 500- 550degC appears to involve significant uptake of oxygen whereas heating at 600degC in argon is just sufficient to allow the oxygen content to get back to O_6 and hence perovskite may form. It is quite likely that if the heating rate is faster than for the above experiments then perovskite may form as the predominant phase throughout the temperature range 450-600degC, in argon atmosphere. The heating rate was limited using platinum grids to 145degC/min since faster heating rates caused the grids to roll up due to differential thermal expansions for the grid and the PZT thin films. Much faster heating rates, up to 125degC/sec, have been achieved for thin films deposited onto platinum electrodes already supported on SiO_2/Si substrates[5,18]. Merklein et al[6] have said that fast firing up to 500degC helps avoid pyrochlore formation. The nucleation site density may also be controlled by adjusting heating rate[6].

It is also worth noting that there is some evidence that excess "PbO" begins to exsolve in the temperature range 450-550degC; see e.g. the spherical nanocrystalline particles attached to the surface of the films in Fig.7. Clearly there is some trade off here, involving "Pb loss" and oxygen stoichiometry changes dependent on the oxygen partial pressure as well as the heating rate. Excess Pb must be removed during RTA but, at the same time, we must maintain the oxygen content at O_5 in order to allow efficient crystallization of perovskite-type PZT. It seems to us that if one can achieve sufficient control of the oxygen content during RTA, by control of the oxygen partial pressure for example, then it may be possible to reduce the amount of excess PbO required.

Finally it is interesting to consider the possibility that some of the Pb ions may achieve valence 4+ during RTA at lower temperatures, say 350-450degC; this follows if the oxygen content exceeds O_6. Thus e.g. the presence of Pb_3O_4 would imply $Pb^{2+}/Pb^{4+} = 2$. This may further complicate the crystallization kinetics, since Pb^{4+} may presumeably occupy octahedrally coordinated B sites of the perovskite structure; note that the ionic radius for six-coordinated Pb^{4+} is 0.078nm, comparable to 0.07nm for Zr^{4+} and 0.063 for Ti^{4+}. If some of the "excess Pb" is incorporated as Pb^{4+} then this will also be exsolved for RTA at sufficiently high temperatures, further complicating the crystallization mechanisms and kinetics.

A systematic study of the effects of heating rate as well as oxygen partial pressure during the RTA crystallization step would be most interesting. The present work allowed inadeqate control over these parameters, certainly for the technique using platinum electron microscope specimen grids. A systematic study of PZT crystallization onto Pt electrodes on SiO_2/Si substrates is presently in progress (Reaney, Brooks, Bursill and Setter, in preparation, 1993).

CONCLUSION.

We have clearly shown that partial pressure of oxygen is an important parameter, which must be controlled, during RTA of PZT ferroelectric thin films. The present results, for thin films deposited directly onto platinum grids, are presently being extended to PZT thin films on standard Pt/TI/SiO_2/Si substrates. This should allow improved switching characteristics to be achieved.

ACKNOWLEDGEMENTS.

This work was supported financially by the Swiss National Funds for Research and the Australian Research Council. we are grateful for the enthusistic support of Prof. Nava Setter and Dr. Ian Reaney, Laboratoire de Ceramique MX-D and Dr Pierre Stadelmann of I2M at EPFL.

REFERENCES.

* Permanent Address: School of Physics, The University of Melbourne, Parkville Vic., 3052, Australia

[1] A.H. Carim, B.A. Tuttle, D.H. Doughty and S.L. Martinez, J. Amer. Ceram. Soc., 74 (1991) 1455-1458.

[2] M. Klee, R. Eusermann, R. Waser and W. Brand, J. Appl. Phys. 72 (1992) 1566-1576.

[3] S. Hirano, T. Yogo, K. Kikuta, Y. Araki, M. Saitoh and S. Ogasahara, J. Amer. Cer. Soc. 75 (1992) 2785-2789.

[4] C.K. Kwok and S.B. Desu, Ceramic Transactions, 25 (1992) 85-96.

[5] I.M. Reaney, K.G. Brooks, R. Klissourska, C. Pawlaczyk and N. Setter, J. Amer. Cer. Soc., in press (1993).

[6] S. Merklein, D. Sporn and A Schonecker, Proc. Symposium N: Ferroelectric Thin Films III, Mat. Res. Soc. Symp. Series, Vol 310, in press (1993) .

[7] J.S. Anderson and N. Sterns, J. Inorg. Nucl. Chem. 11 (1959) 272-285.

[8] I. Kondo, T. Yoneyama and O. Takeuaka, J. Vac. Sci. Technol. A10 (1992) 3436.

[9] C.A. Sorrel, J. Amer. Cer. Soc. 56 (1973) 613-618.

[10] P.V. Kovtunenko, Ya.L. Kharif, I.L. Nesterova and L.P. Stupak, Russian J. Phys. Chem. 53 (1979) 2000-2003.

[11] R.A. McCauley, J.Appl.Phys. 51 (1980) 290-294.

[12] D.P. Martin, Phys. Chem. Glasses 6 (1963) 143-146.

[13] F. Chaput, J-P. Boilot, M. Lejeune, R. Papiernik, L.G. Hubert-Pfalzgraf, J. Am. Cer. Soc. 72 (1989) 1335-1357.

[14] K.D. Budd, S.K. Dey and D.A. Payne, Brit.Ceram. Proc., 36 (1985) 107-121.

[15] T.W. Dekleva, J.M. Hayes, L.E. Cross and G.L. Geoffrey, J. Amer. Ceram. Soc., 71 (1988) C280-282.

[16] C.K. Kwok and S.B. Desu, Appl. Phys. Letts. 60 (1992) 1430-1432.

[17] C.V.R. Vasant Kumar, R. Pascual and M Sayer, J. Appl. Phys. 71 (1992) 864-874.

[18] I.M. Reaney, K.G. Brooks, L.A. Bursill and Nava Setter, in preparation, (1993).

Figure Captions.

Fig.1(a). Plot of PbO/Pb_3O_4 equilibrium solidus line as a function of the partial pressure of oxygen and temperature. Note that to retain $PbO_{1.00}$ for 300-600degC requires $pO_2 < 10^{-3}$atm.

Fig.1(b). Plot of the solubility of the excess oxygen x_O in PbO_{1+xO} as a function of temperature. Note that x_O ranges from 0.01 to 0.04 as the temperature increases from 300degC to 700degC, assuming the partial pressure of oxygen is controlled to track the PbO/Pb_3O_4 equilibrium solidus.

Fig.2. (a) Electron diffraction pattern and (b) HRTEM image of specimen A, after RTA at 700degC. Note randomly-oriented nanocrystalline pyrochlore structure, grain size approx 5-8nm.

Fig.3. (a) Electron diffraction pattern and (b) HRTEM image of specimen B, as- pyrolyzed at 350degC. Note purely amorphous nature of the structure and the overlap of the diffuse ring pattern with the pyrochlore ring pattern (cf. Figs.2a,5a).

Fig.4. (a) Electron diffraction pattern and (b) HRTEM image of specimen C, after RTA at 600degC in flowing argon. Note predominance of perovskite ring pattern in (a) and the relatively large crystallite of perovskite PZT; with apparent disorder in the perovskite structure (b).

Fig.5. (a) Electron diffraction pattern and (b) HRTEM image of specimen D, after RTA at 600degC in flowing oxygen. Note poorly crystallized pyrochlore structure (cf. Fig.2).

Fig.6. (a) Electron diffraction pattern and (b) HRTEM image of specimen E, after 420degC pyrolysis in air; there is no evidence for crystallization. (c) shows development of rafts consisting of atomic layers of perovskite on the surface after 20 minutes observation in the electron beam; 3nm nanocrystals of "PbO" also appeared.

Fig.7. (a) Electron diffraction pattern from specimen G after 450degC RTA in argon; note perovskite-type spot patterns on pyrochlore-type diffuse ring pattern. (b) shows perovskite-type spot patterns on as-pyrolyzed type diffuse ring pattern (cf. Fig.3). (c) shows HRTEM image of perovskite-type PZT; note "PbO" nanocrystals which decorate the surface of the crystal.

Fig.8. (a,b) show electron diffraction patterns of specimen H after RTA at 500degC in argon; note pyrochlore- and as-pyrolyzed-type diffuse ring patterns, as for Fig.7(a,b), but the spot patterns changed to pyrochlore-type.

Fig.9. Electron diffraction pattern from specimen I after RTA at 550degC in argon; note sharp ring pattern characteristic of relatively well-crystallized nanocrystalline pyrochlore-type PZT.

Fig.10. (a,b) Electron diffraction patterns from specimens J and K, after RTA at 600degC and 450degC respectively in forming gas; in both cases the diffuse ring patterns are essentially identical to those of the original as-pyrolyzed specimen (cf. Fig.3).

Table 1: Pyrolysis and Rapid Thermal Annealing Conditions

Specimen	Pyrolysis (s/C)	Heating Rate (C/min)	Soak (sec/C)	Atmosphere
A	Air Dried	135	60/700	Air
B	60/350	not	annealed	Air
C	60/350	145	60/600	Argon
D	60/350	145	60/600	Oxygen
E	60/420	not	annealed	Air
F	60/350	145	60/400	Argon
G	60/350	145	60/450	Argon
H	60/350	145	60/500	Argon
I	60/350	145	60/550	Argon
J	60/350	145	60/600	Forming Gas
K	60/350	145	60/450	Forming Gas

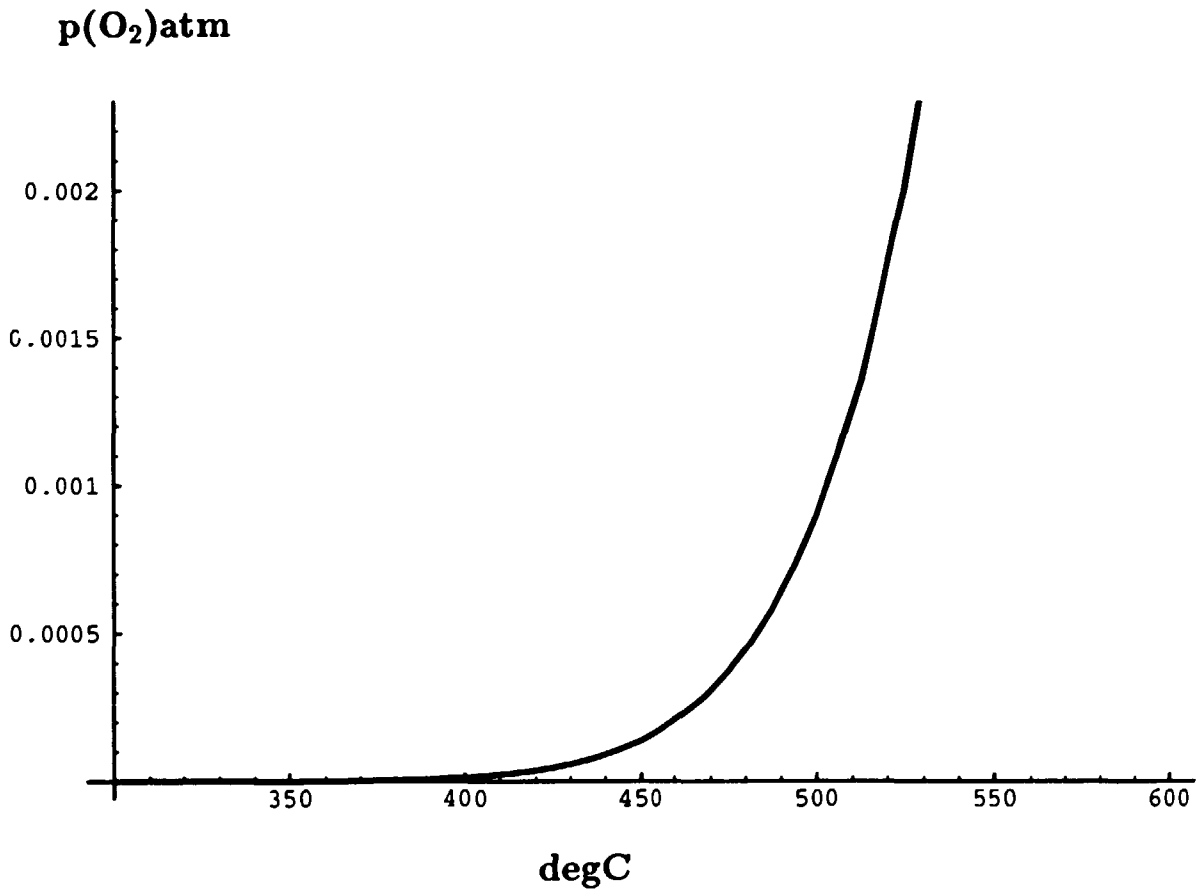

FIG. 1a

Burrill + Brooks, 1993
J. Appl. Phys.

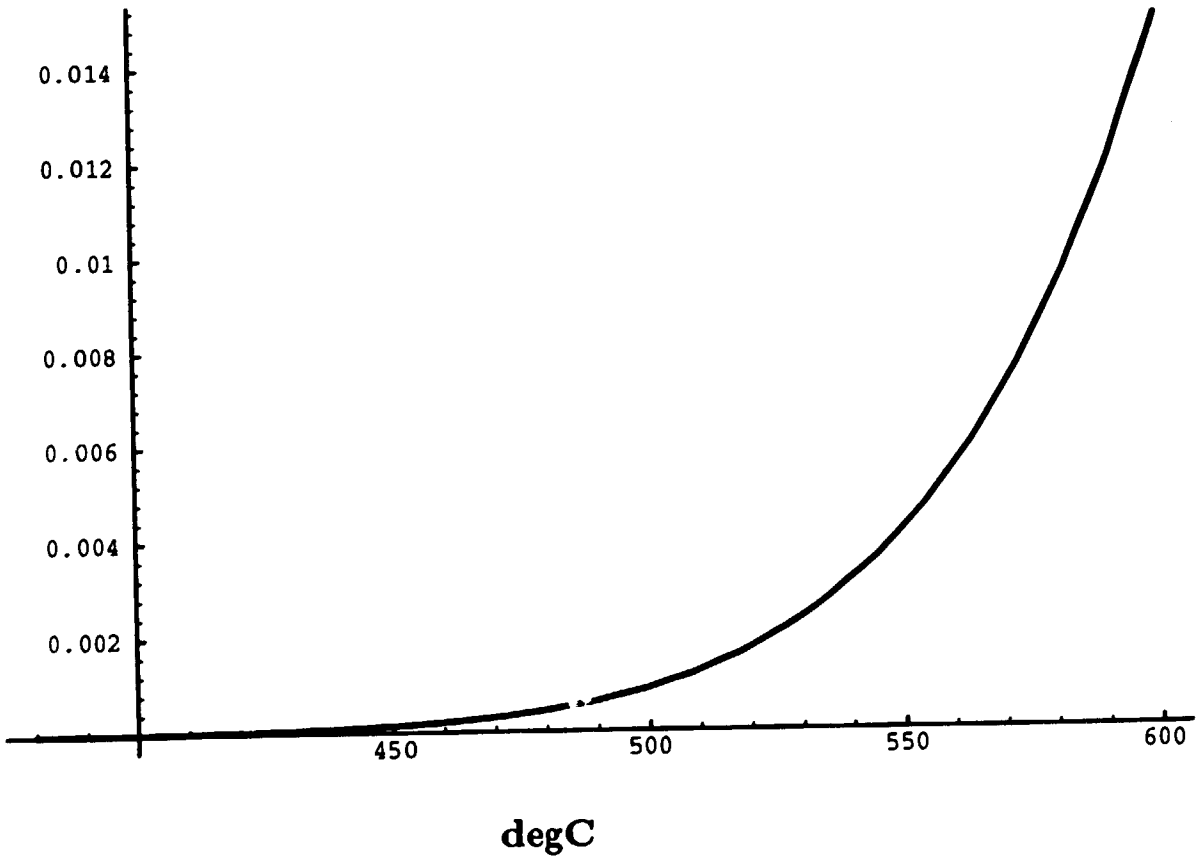

FIG. 1b

Burrill, Brooks 1963
J. Appl. Phys.

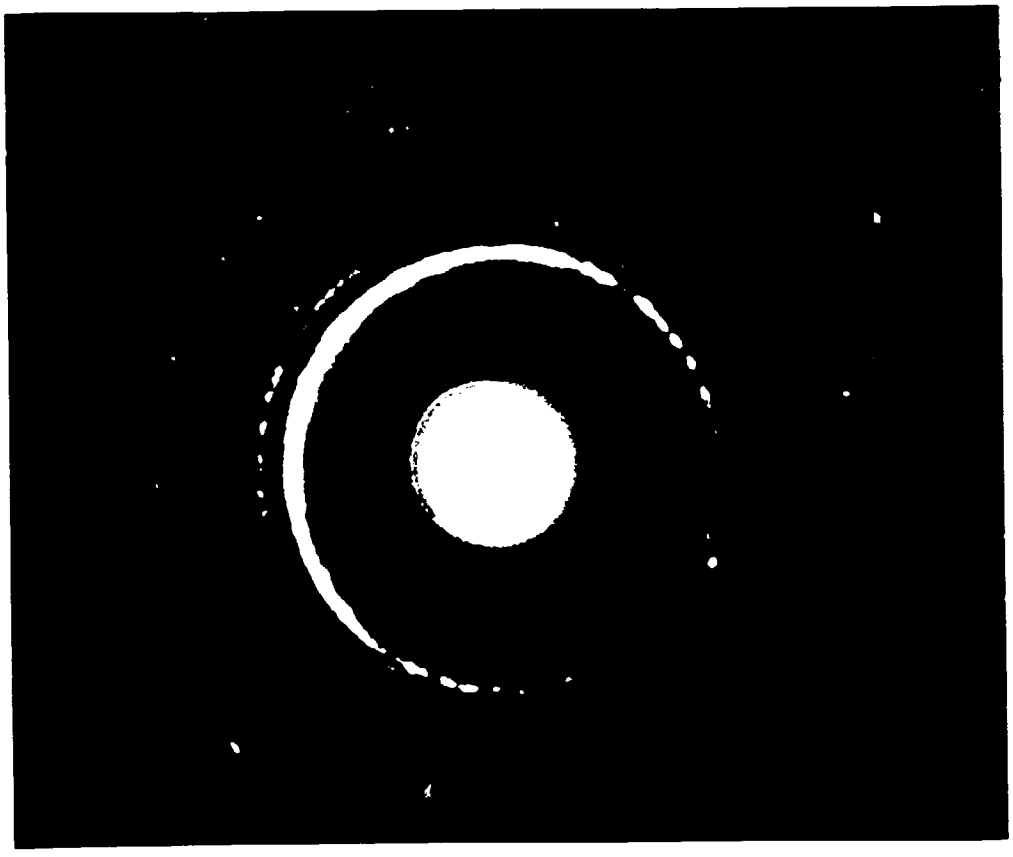

a

b

1nm

FIG. 2

Ewald + Brooks 1992 J. Appl. Phys.

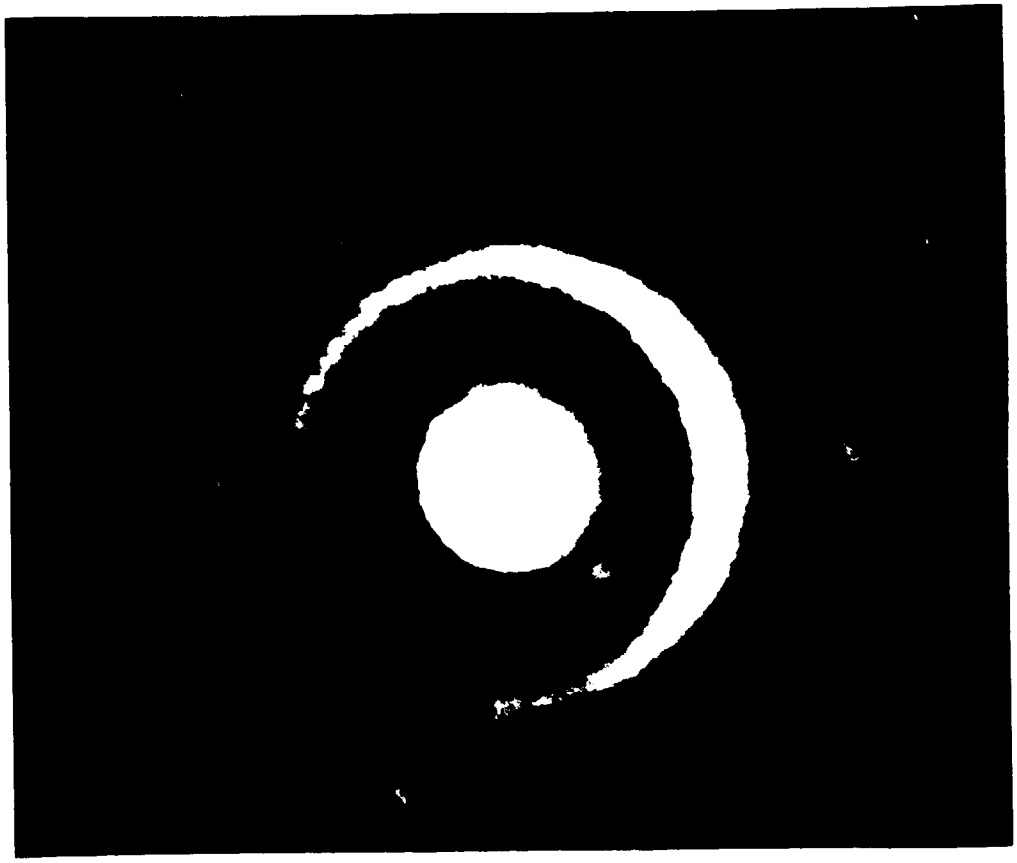

a

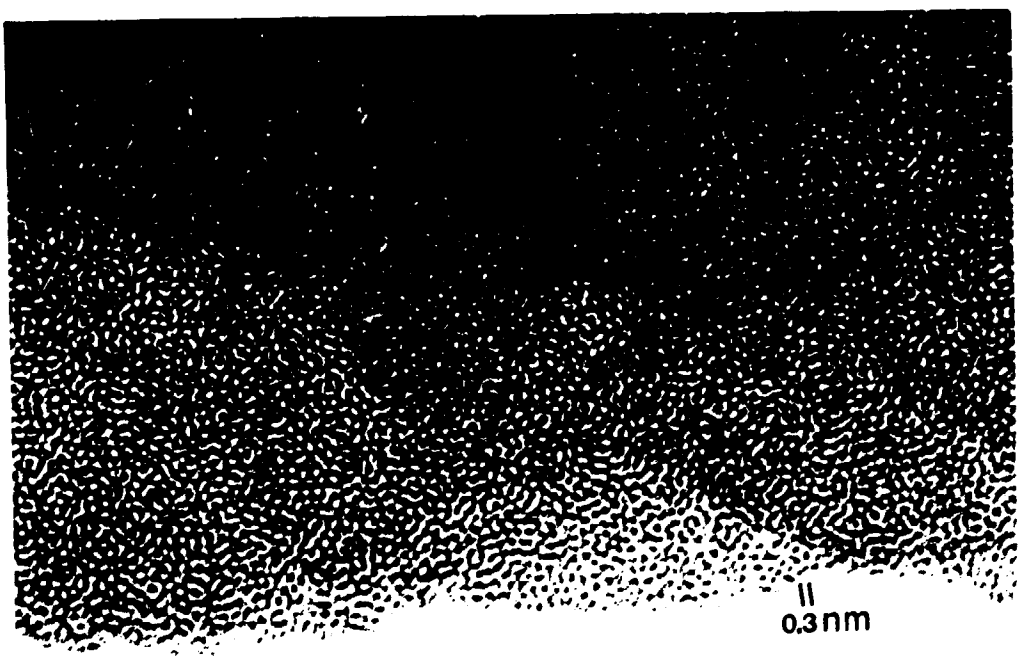

b

FIG. 3

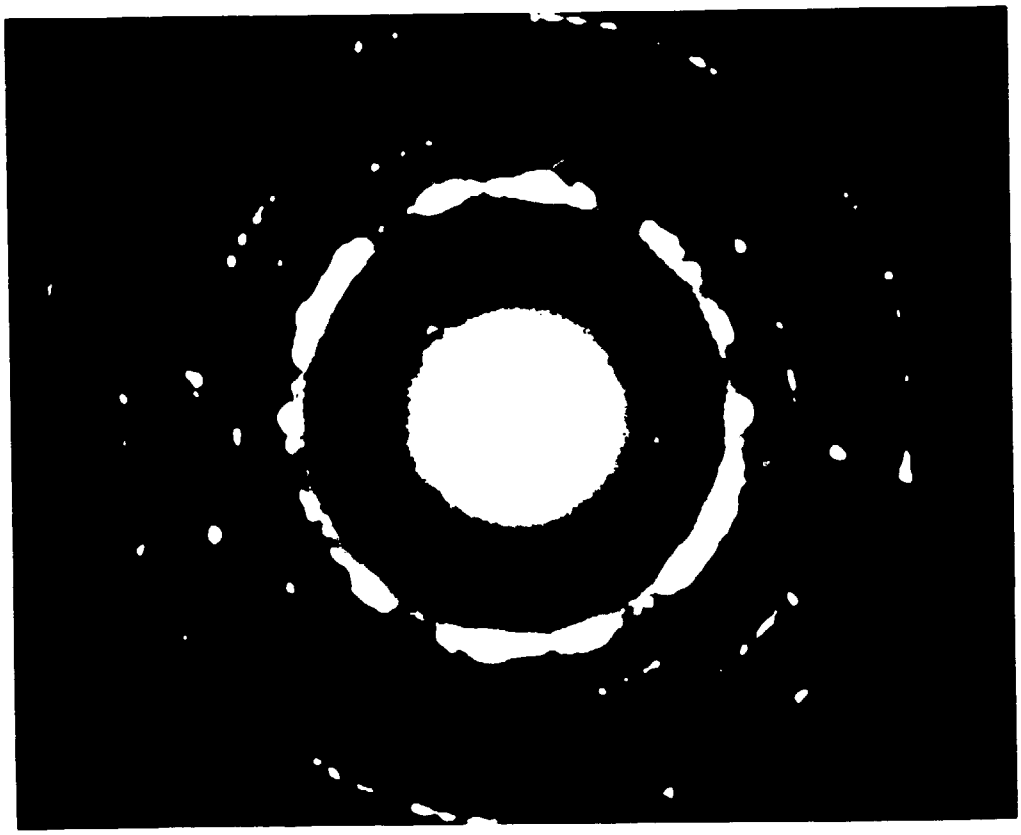

a

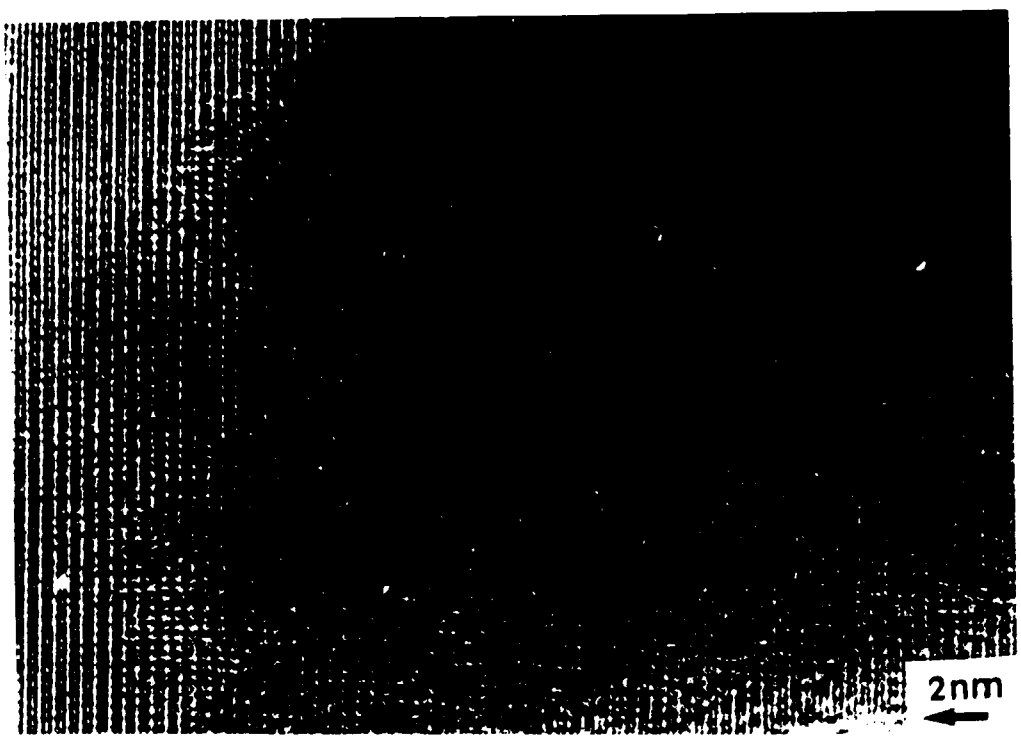

b

FIG. 4

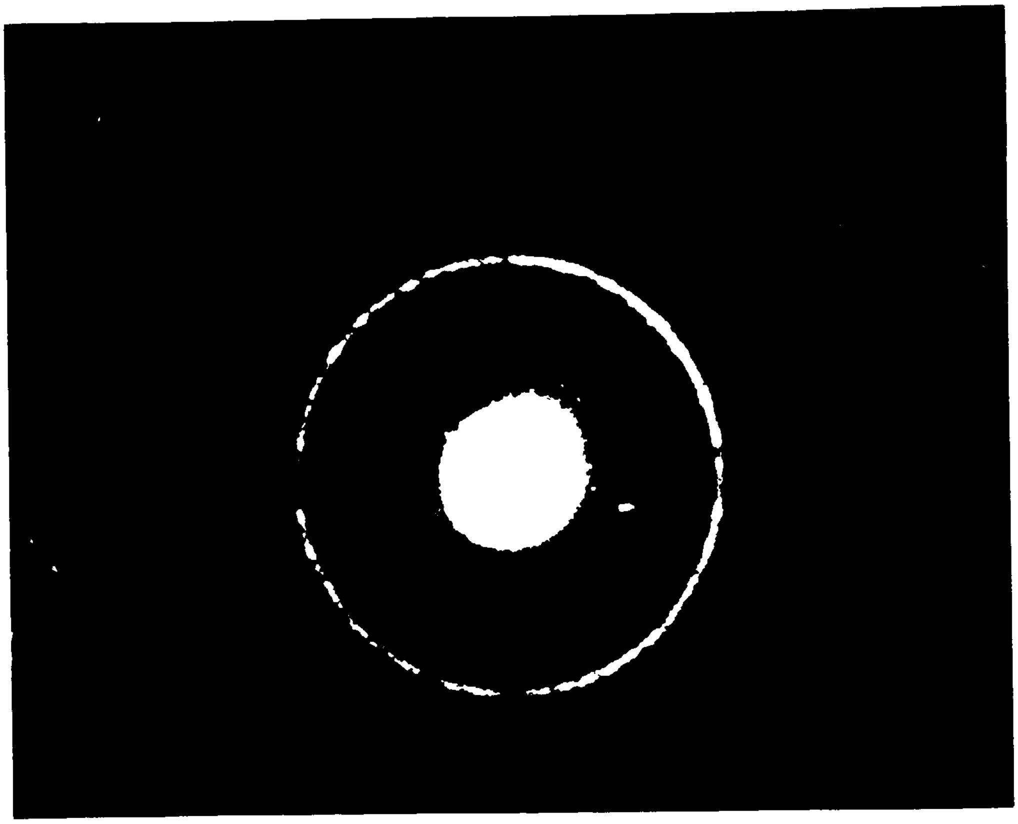

a

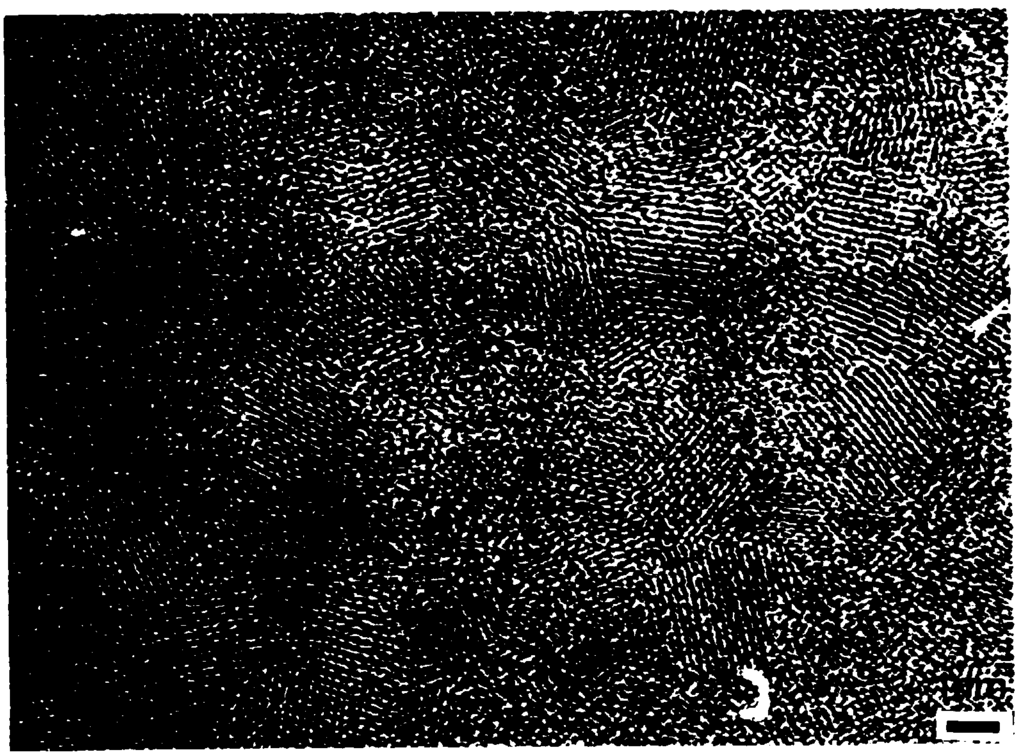

b

FIG. 5

Burrell & Brooks, 1953
J. Appl. Phys.

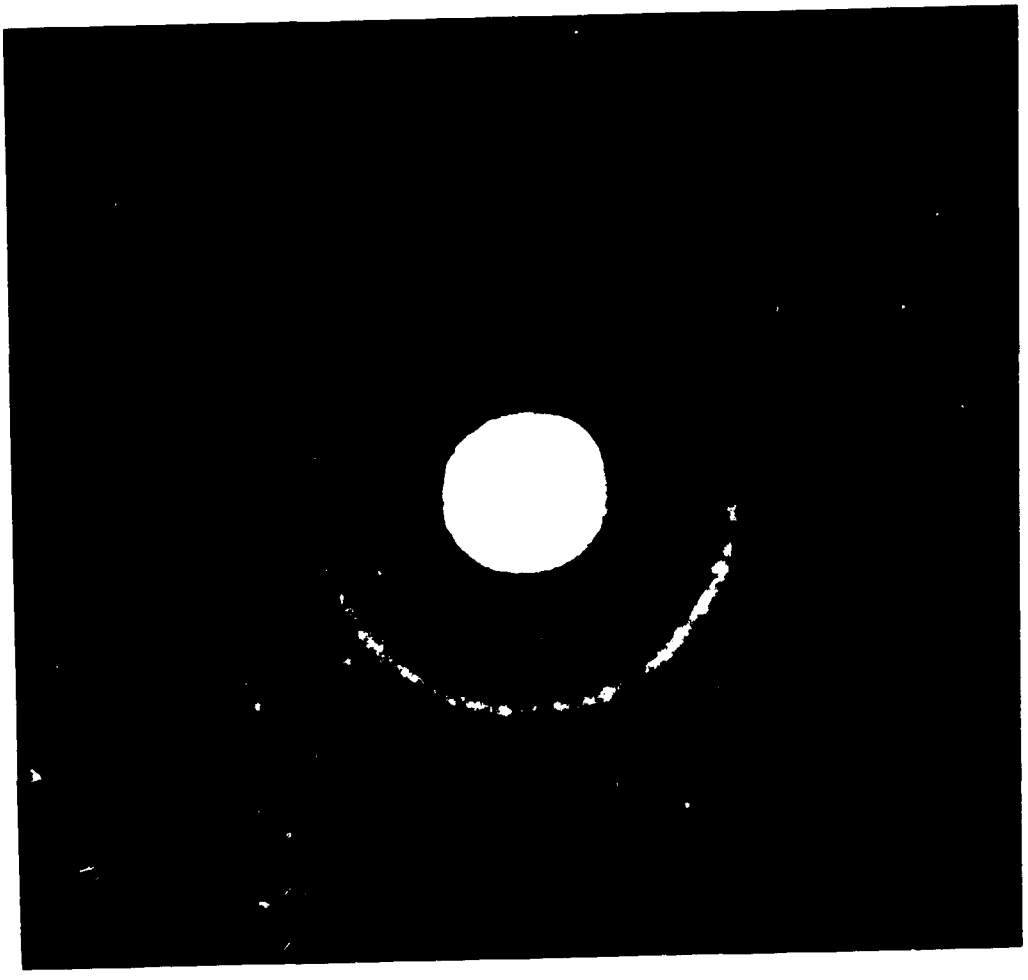

a

Fig.6

Burrell, Brooks, 1993
J Appl Physics

b c

Fig.6

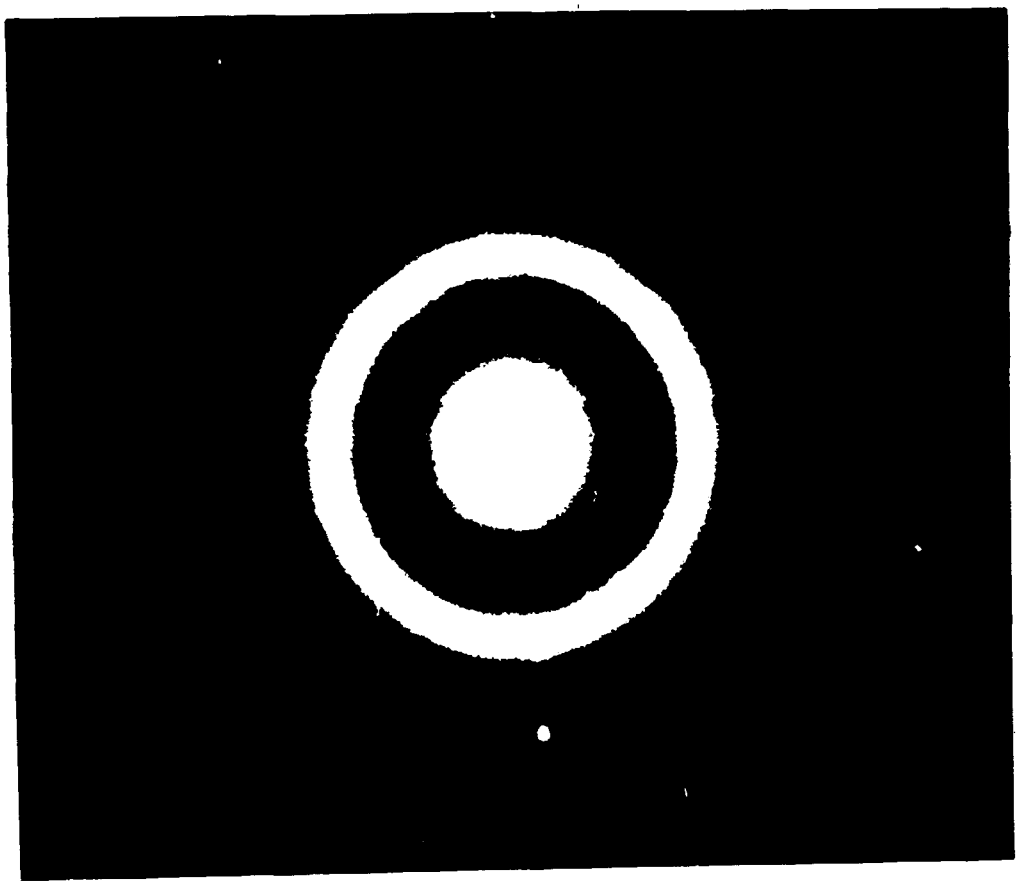

a

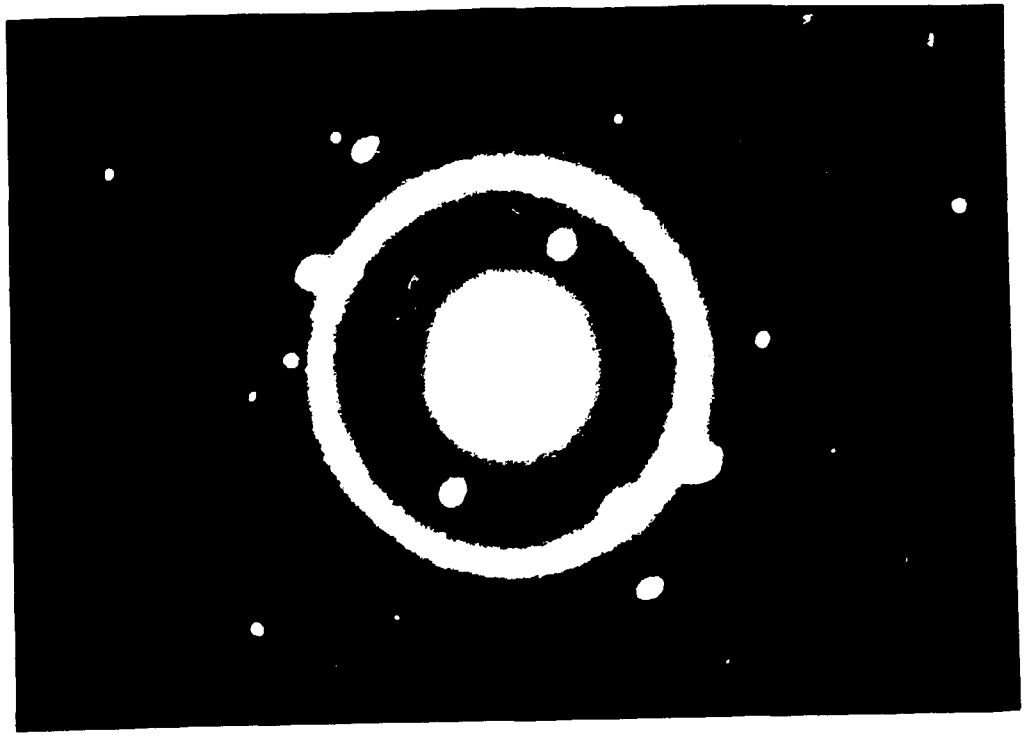

b

Fig.7

Bunsell & Brooks, 1993
J. Appl. Phys.

c

Fig.7

Bunch + Brooks 19..
T Appl Phys

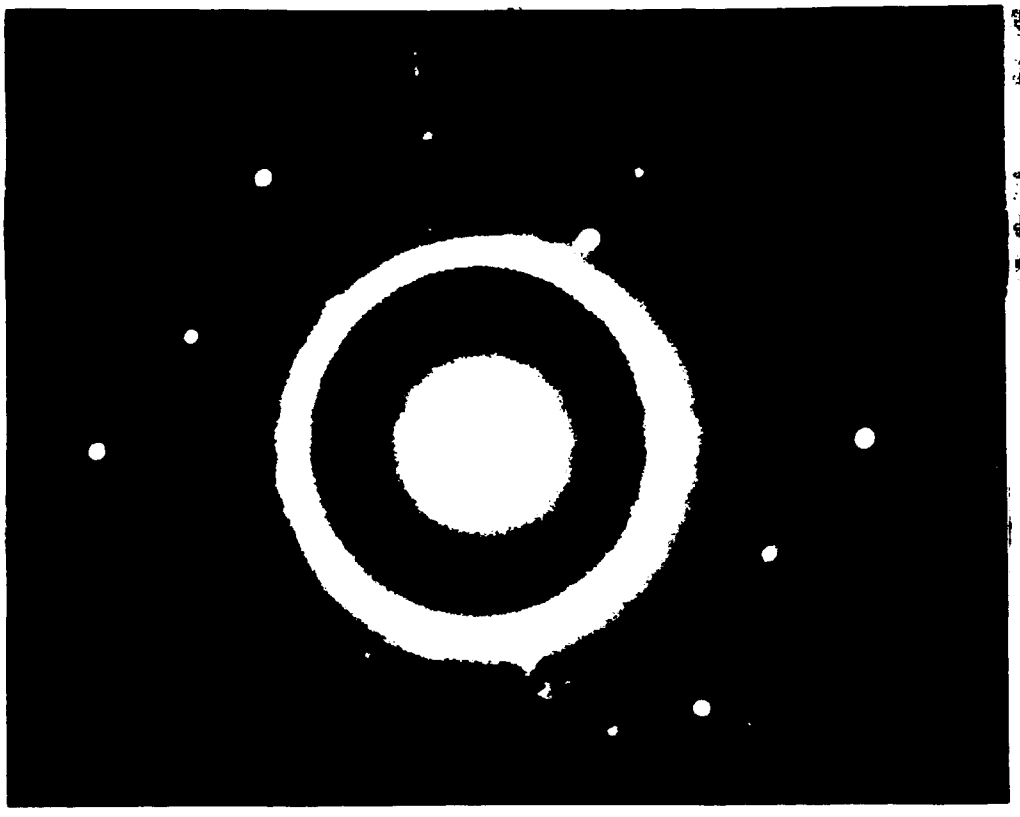

a

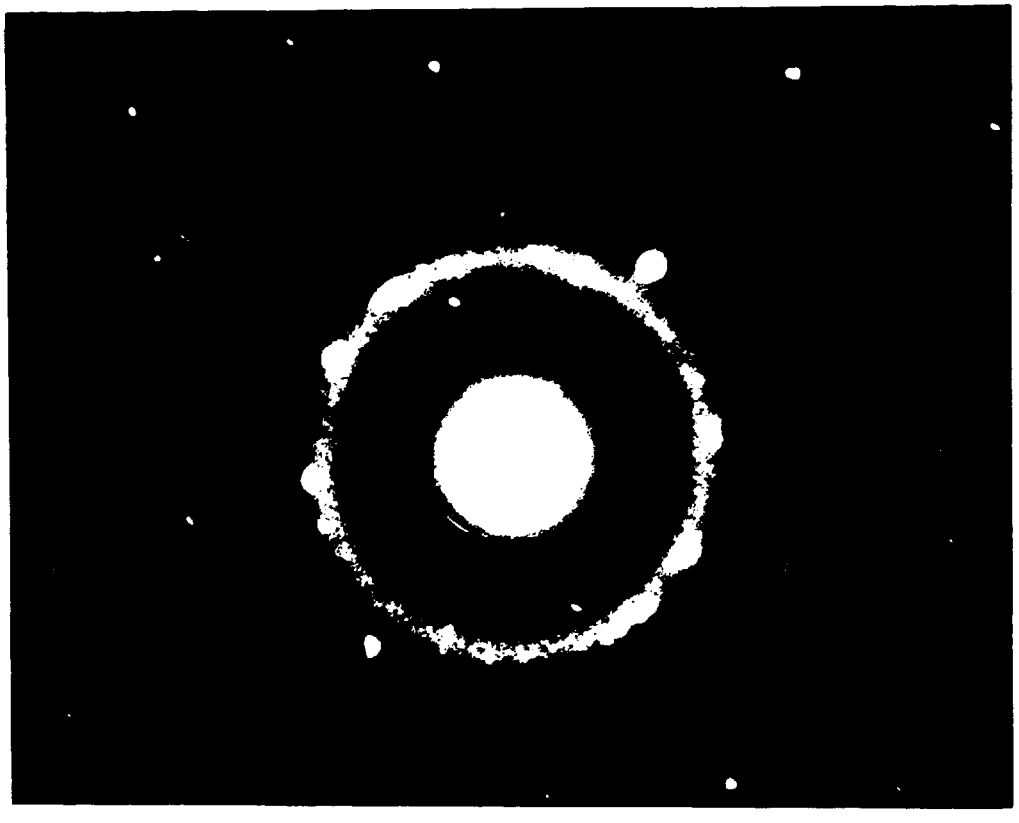

b

Fig.8

Bunshi : Brooks 1993

J. Appl. Phys.

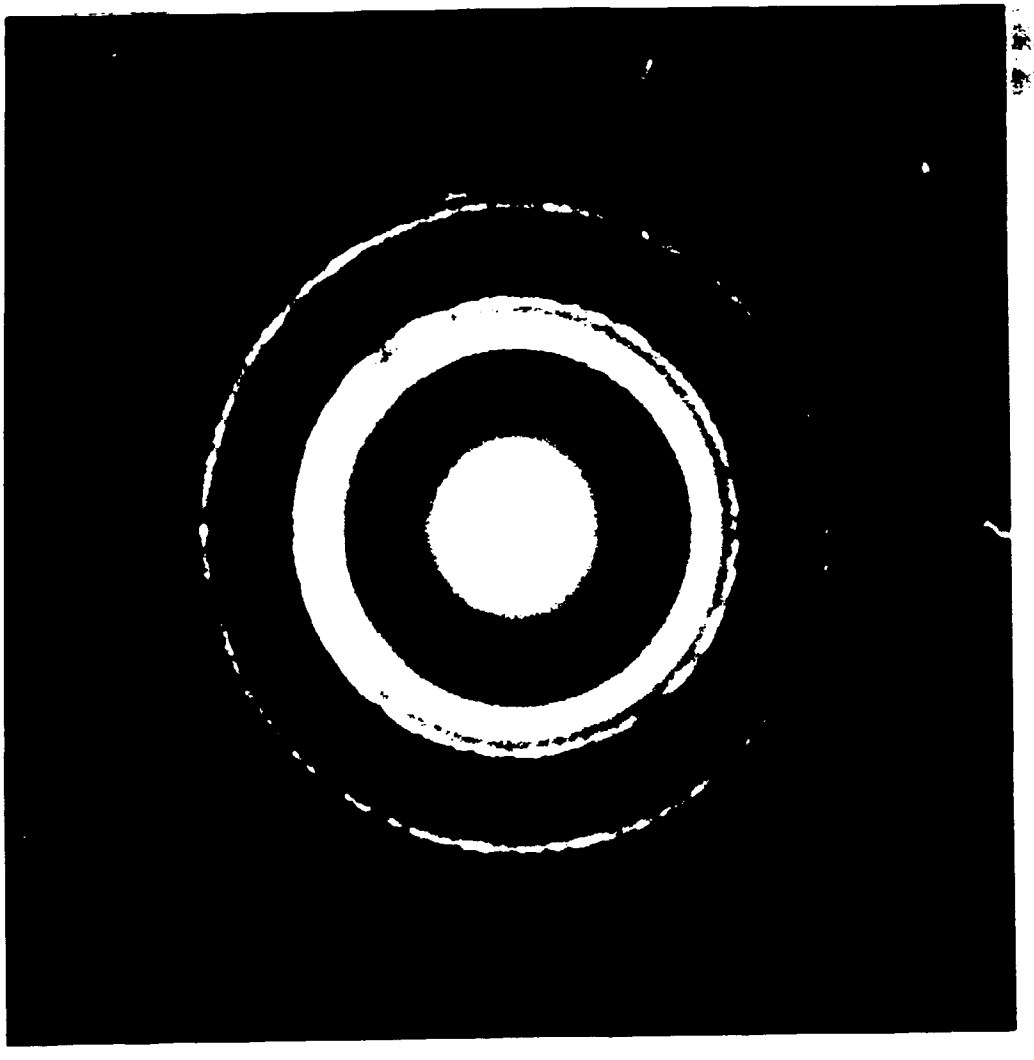

c

Fig.9

Bunsell + Brooks, 1993
J. Appl. Phys.

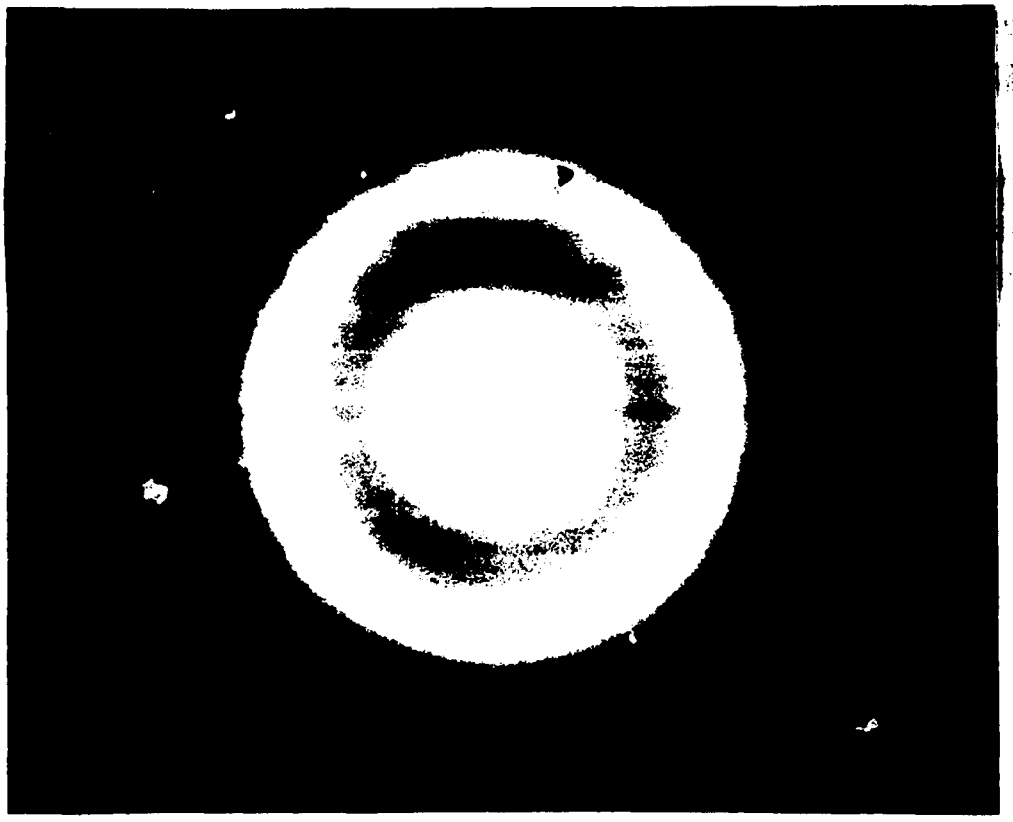

a

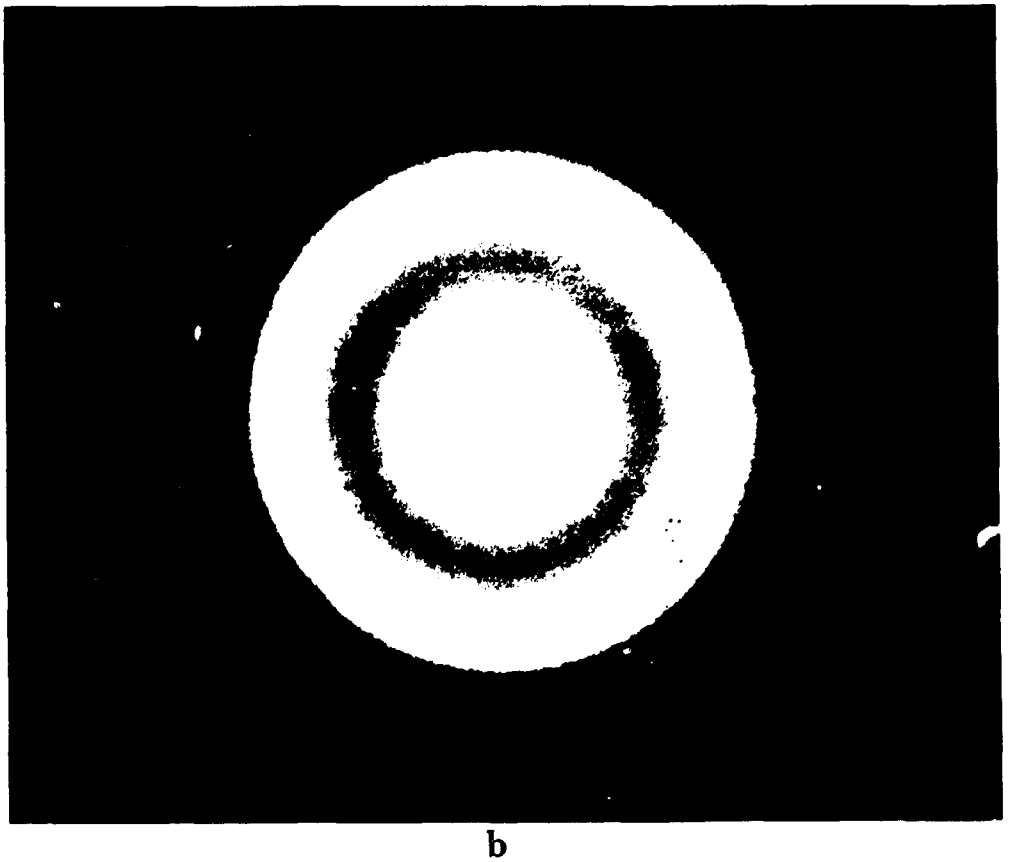

b

Fig.10

Burrill & Brooks, 1949
J. Appl. Phys.